Supporting Information

Aqueous Phase Behaviour of Choline Carboxylate Surfactants – Exceptional Variety and Extent of Cubic Phases

Regina Klein,[a] Gordon J. T. Tiddy,[b] Eva Maurer,[a] Didier Touraud,[a] Jordi Esquena,[c] Olivier Tache,[d] Werner Kunz[a]*

Table of Content

I. Density and determination of the molar volume of ChC*m* surfactants

Densities of aqueous choline carboxylate solutions were determined at 25°C by a vibrating tube densimeter (Anton Paar DMA 60). The experimental derived values are listed in Table 1.

ChC12		ChC14		ChC16		ChC18	
wt%	ρ / g L^{-1}	wt%	ρ / g L^{-1}	wt%	ρ / g L^{-1}	wt%	ρ / g L^{-1}
1.00	997.09	1.00	996.78	1.00	996.65	1.00	996.62
2.49	996.79	2.49	996.32	2.50	996.00	2.49	995.82
5.00	996.33	4.99	995.44	4.99	995.05	5.00	994.43
7.48	995.89	7.46	994.71	7.50	993.82	7.48	993.13
9.98	995.40	10.00	993.91	10.00	992.95	9.55	992.11
12.50	994.97	12.46	993.14	12.47	991.77	12.49	990.62
14.95	994.45	15.00	992.32	15.00	990.68	14.98	989.47
17.44	994.04	17.46	991.54	17.51	989.78	17.48	988.07
20.00	993.56	20.00	990.87			20.01	986.83

Table 1. Density data of ChC*m* surfactants at 25°C.

With the known molar masses of surfactants and water, the total volume (V_{total}) of solution with regard to 1 mol H_2O can be calculated. And with n_s and V_S as number of moles and molar volume of surfactant, V_{total} is defined as:

$$V_{total} = n_{H2O}V_{H2O} + n_S V_S$$

Consequently, V_S can be derived by the plot of V_{total} versus n_s (Figure 1).

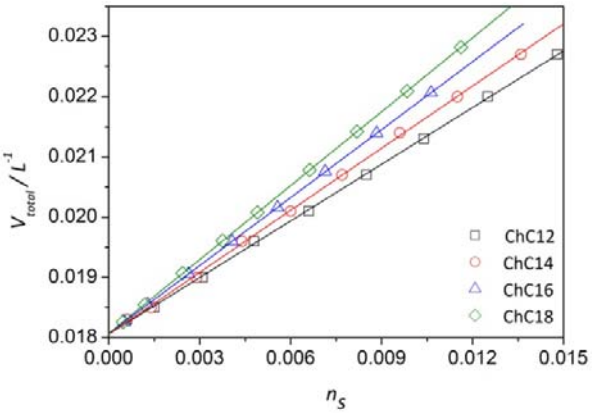

Figure 1. Plot of the total volume V_{total} at 25°C versus the number of moles of ChC*m* surfactants according to Equation (1).

As obvious from Figure 1, V_S is constant over the investigated concentration region and can thus be obtained by the slope of a linear regression. Thereby, the y-axis interception represents the molar volume of water, since V_{total} was calculated for n_{H2O}= 1 mol. The results of the linear regression are listed in Table 2. V_{H2O} agrees well to the literature. Further, V_S increases in average by a factor of 0.0165 L mol^{-1} (= 27.4 Å^3) per additional CH_2 group, which correspond approximately to the value predicted by Tanford (26.9 Å^3).[1]

	V_S / L mol^{-1}	V_{H2O} / L mol^{-1}
ChC12	0.310	0.0181
ChC14	0.343	0.0181
ChC16	0.376	0.0181
ChC18	0.409	0.0181

Table 2. Results of the linear regression according to Figure1, revealing the molar volumes of choline surfactants and water at 25°C.

II. Penetration scan images of ChC*m* surfactants at various temperatures

II.1. ChC14

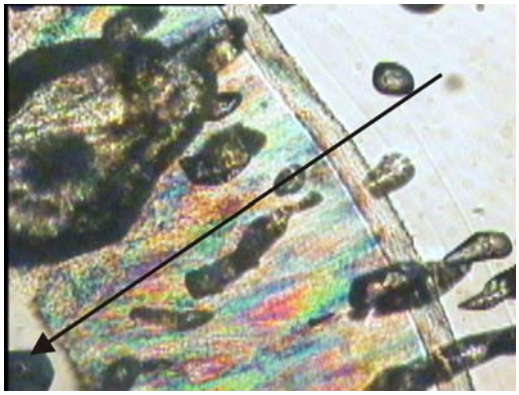

Figure 2. Penetration scan image of ChC14 at 25°C and 100x magnification, showing towards higher soap concentrations (as assigned by the arrow) the following mesophases: L_1, I_1', I_1'', H_1, and V_1.

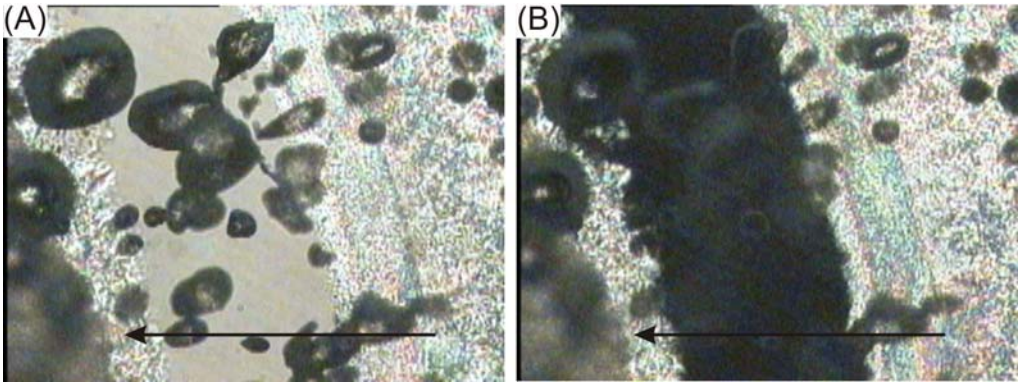

Figure 3. Penetration scan image of ChC14 in the more concentrated surfactant region at 50°C and 100x magnification without (A) and with (B) crossed polarizers. From the right to the left (increasing surfactant concentration) H_1, V_1, L_α and a solid birefringent region can be identified.

II.2. ChC16

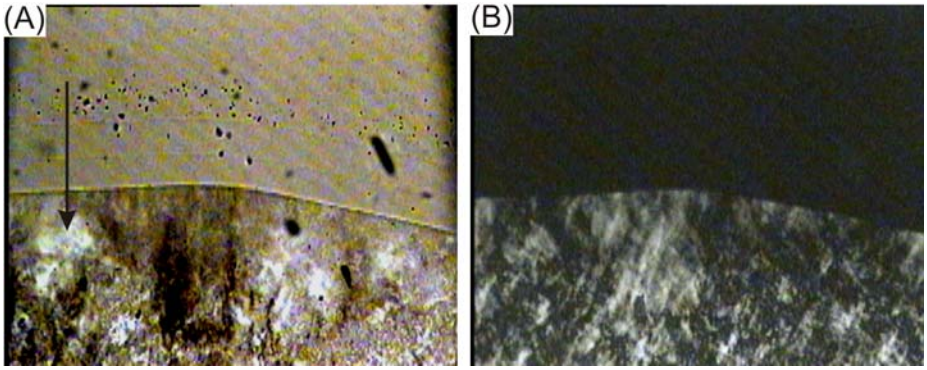

Figure 4. Penetration scan of ChC16 at 25°C and 100x magnification without (A) and with (B) crossed polarizers, showing from the top to the bottom L_1, I_1', I_1'' and H_1.

II.3. ChC18

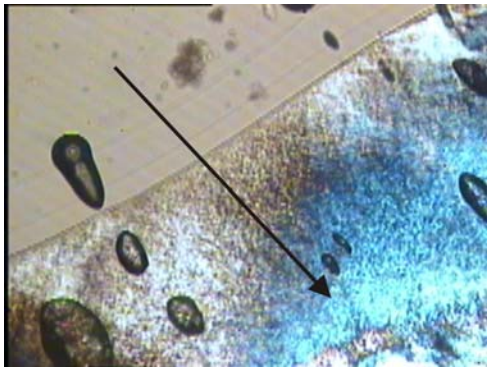

Figure 5. Penetration scan photograph of ChC18 at 40°C and 100x magnification. With increasing soap concentration (as pointed by the arrow) the following mesophases could be identified: L_1, I_1', I_1'' and H_1.

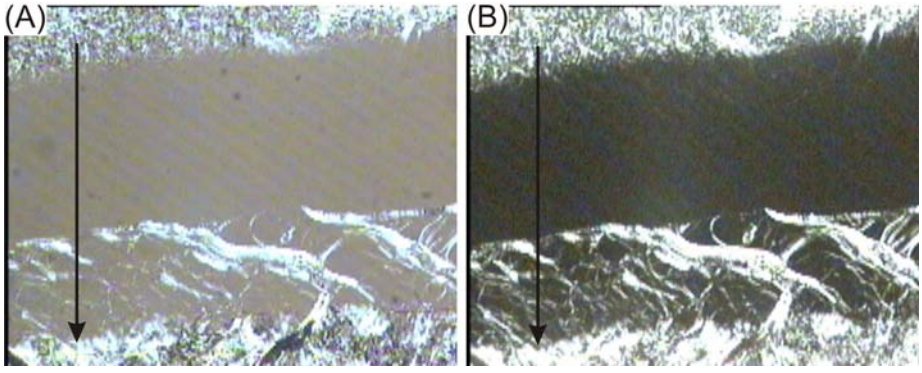

Figure 6. Penetration scan of ChC18 in the more concentrated surfactant region at 59°C and 100x magnification (with (A) and without (B) crossed polarizers), showing from the top to the bottom the following mesophases: H_1, V_1, L_α and L_β.

III. SAXS experimental

SAXS measurements were performed on three different devices of various labs due to limited facilities and different demands such as varying required scattering angles, temperature controlling or the recording of two dimensional X-ray patterns. The assignment of the investigated samples to the respective experimental setups can be found in Table 3 and Table 4.

(A) SAXS setup supplied by the laboratories of LIONS/CEA, Saclay (France):

X-ray radiation with wavelength λ= 1.54 Å is provided by a copper rotating anode operated at 3 kW equipped with a multilayer Xenocs mirror as monochromator and a three slit collimation system. The scattered X-rays were detected by a two dimensional automatic image plate system (Mar300) from Marresearch. Calibrations were done by measuring standards such as octadecanol, iron, water and Lupolen. With a sample to detector distance of 122 cm the accessible *q*-range was 0.3-6.3 nm^{-1}. More details regarding the experimental setup can be found in the literature.[2, 3] Samples were enclosed between Kapton sheets with sample thicknesses of 1 mm and 1.5 mm. Acquisition times varied between 900-7200 s. Radial averaging was performed with ImageJ Software. On this device, ChC12 and ChC16 were fully characterized and ChC18 to a great extent.

(B) SAXS instrument at the institute for Advanced Chemistry of Catalonia, Barcelona (Spain):

Small angle X-ray scattering data were recorded using a S3 MICRO instrument (Hecus X-ray Systems, Graz, Austria) equipped with a sealed copper anode providing Cu-K_α radiation with λ= 1.54 Å. The beam is focused using a Genix microfocus X-ray source and a Fox 2D point-focusing element (both from Xenocs, Grenoble), reducing the beam area to approximately 0.04 mm^2. The detection system is composed of two linear position sensitive detector (PSD-50M, Hecus, Graz, Austria), which allows the simultaneous determination of small and wide angles, covering q-values between approximately 0.2 and 5.9 nm^{-1}, and between 13 and 19 nm^{-1}, respectively. Exact *d* spacing values were achieved by calibration with silver behenate for small angles and by *p*-bromobenzoic acid for large angles.[4-6] Samples were employed in a paste cell of approximately 1 mm thickness sealed with plastic foil (Kallebrat Folie, Kalle GmbH, Germany). Investigated temperatures ranged from 0°C until 90°C with acquisition times of 900-1800 s. Primarily ChC14 was characterized on this setup.

(C) SAXS apparatus at the Max-Planck institute Potsdam (Germany):

This homebuilt instrument consists of a rotating anode (Fr591, Bruker-Nonius, Netherlands) with point collimation and a two dimensional Mar CCD Detector (Mar 165), which posses a resolution of 2048 x 2048 pixels with a pixel size of 79 µm. Calibration was performed by measuring silverbehenate.[4, 6] With a sample to detector distance of 74.1 cm, a *q*-range of 0.6-4.6 nm^{-1} was attained. Primary data were processed with ImageJ Software.

ChC12			ChC14		
wt%	T /°C	SAXS-setup	wt%	T /°C	SAXS-setup
30.0	25	A	29.0	25	C
32.9	25	A	34.9	25	C
35.1	25	A	37.4	25	C
37.9	25	A	40.9	25	C
40.1	25	A	45.0	25	B
45.0	25	A	50.6	25	B
47.2	25	A	56.0	25	B
49.7	25	A	61.0	25	B
55.1	25	A	65.0	25	B
60.2	25	A	70.2	25	B
65.5	25	A	75.4	25	B
69.9	25	A	79.8	25	B
74.7	25	A	79.8	60	B
79.9	25	A	83.3	25	B
83.8	25	A	85.5	20	B
86.9	25	A	90.4	25	B
89.5	25	A	93.2	35	B
91.5	25	A	95.1	45	B
94.0	25	A	95.1	80	B
97.5	60	A	97.5	80	B

Table 3. Assignment of ChC12 and ChC14 samples, which has been investigated by SAXS, to the respective experimental X-ray setup.

ChC16			ChC18		
wt%	T /°C	SAXS-setup	wt%	T /°C	SAXS-setup
30.1	25	A	34.7	60	A
34.8	25	A	45.2	60	A
40.1	25	A	50.3	60	A
45.2	25	A	60.0	50	C
49.7	25	A	69.9	50	C
54.7	25	A	75.7	70	C
59.6	25	A	79.8	70	C
64.4	25	A	85.7	70	C
69.7	25	A	90.2	70	C
75.3	50	A	96.0	70	C
79.3	50	A			
85.5	50	A			
89.3	50	A			
92.0	60	A			
94.0	50	A			
95.3	60	A			
97.5	70	C			

Table 4. Assignment of ChC16 and ChC18 samples, which has been investigated by SAXS, to the respective experimental X-ray setup.

IV. SAXS spectra

In the following the SAXS spectra obtained on each compound are presented. If not otherwise outlined, the temperature is 25°C. The spectra are approximately ordered to the respective mesophases. The details and the exact assignment to the various liquid crystalline structures can be found in following chapter (V. X-ray diffraction data).

IV.1. ChC12

IV.1.1. Discontinuous cubic I_1' and I_1'' (P*m3n*)

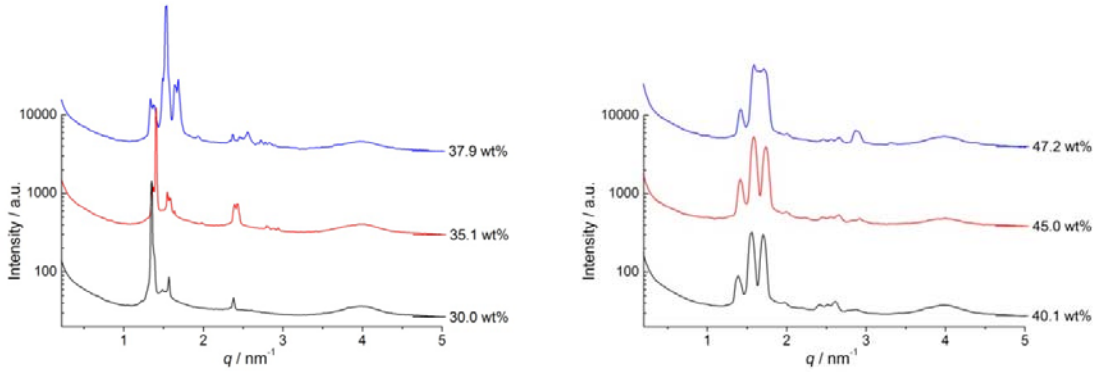

IV.1.2. Hexagonal phase H_1

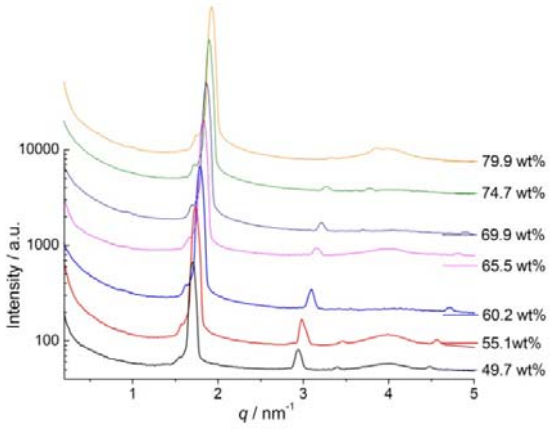

IV.1.3. H_1 – V_1 boundary – intermediate phase?

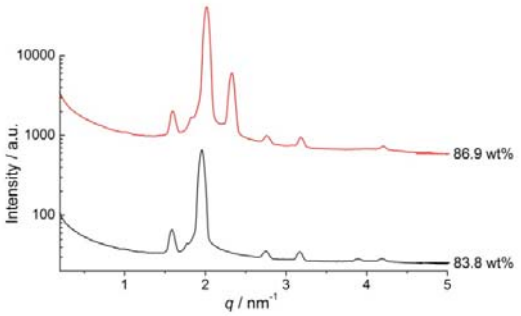

IV.1.4. Bicontinuous phase V_1 with I*a3d* structure

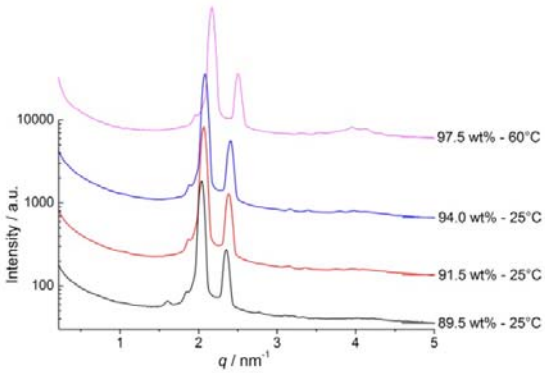

For L_α of ChC12, no X-ray data are available at the moment owing to the particular narrowness of the phase region in this case and since, in addition, it only occurs at elevated temperatures.

IV.2. ChC14

IV.2.1. Discontinuous cubic I_1‘ and I_1‘‘ (P*m3n*)

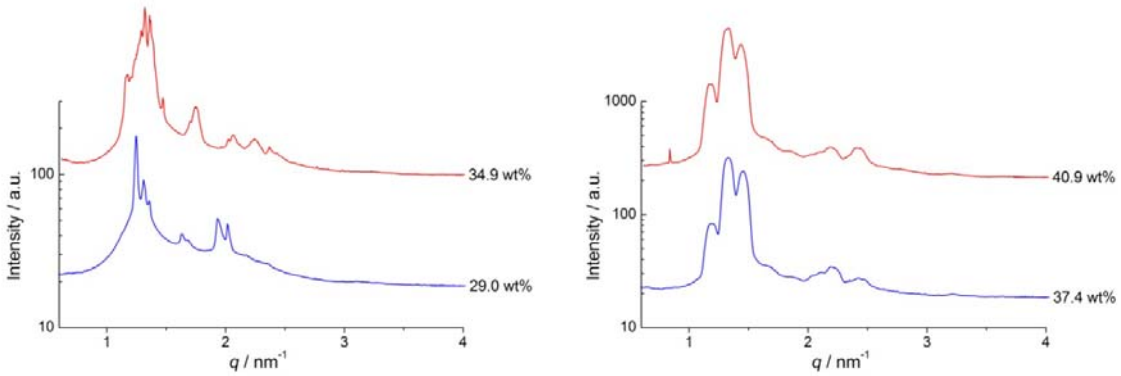

IV.2.2. Hexagonal phase H_1

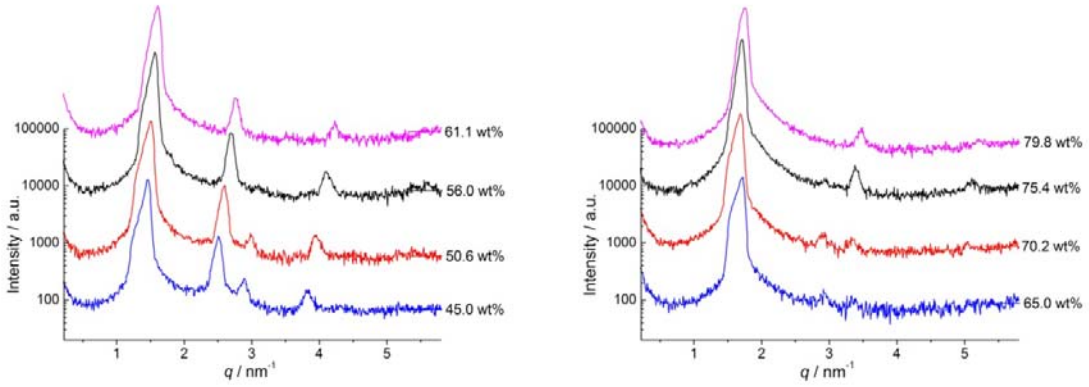

IV.2.3. Bicontinuous phase V_1 with I*a3d* structure

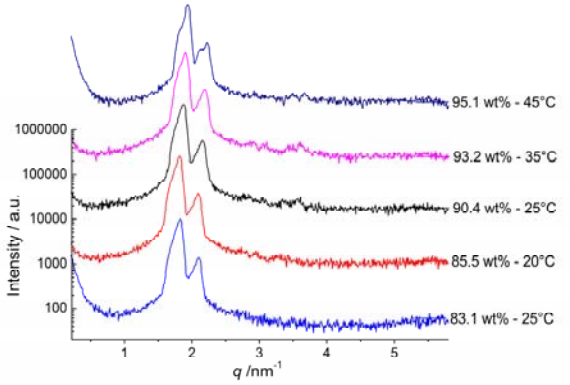

IV.2.4. Lamellar phase L_α

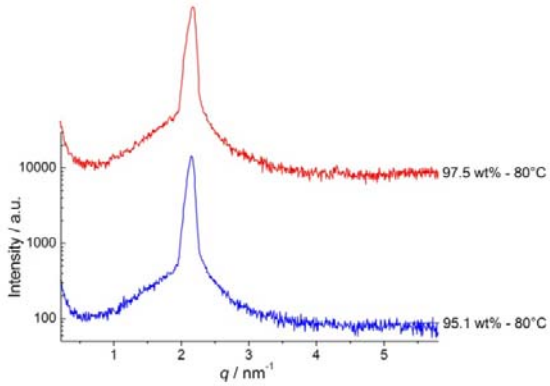

IV.3. ChC16

IV.3.1. Discontinuous cubic I_1' and I_1'' (P*m3n*)

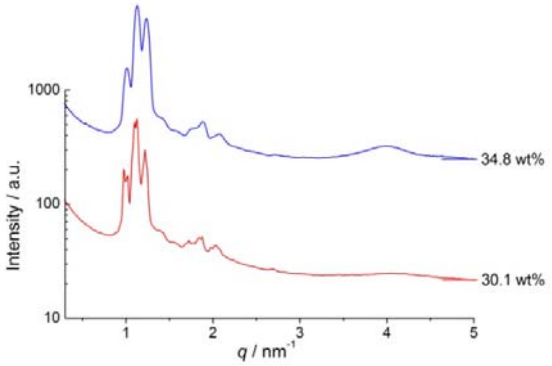

IV.3.2. Hexagonal phase H_1

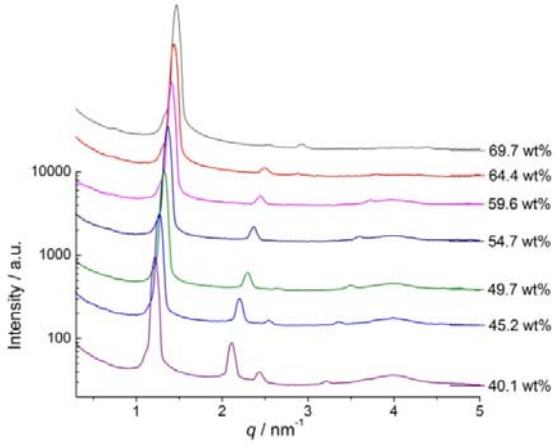

IV.3.3. H_1 – V_1 boundary – intermediate phase?

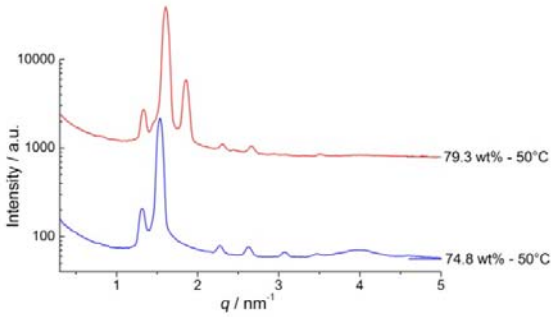

IV.3.4. Bicontinuous phase V_1 with I*a3d* structure

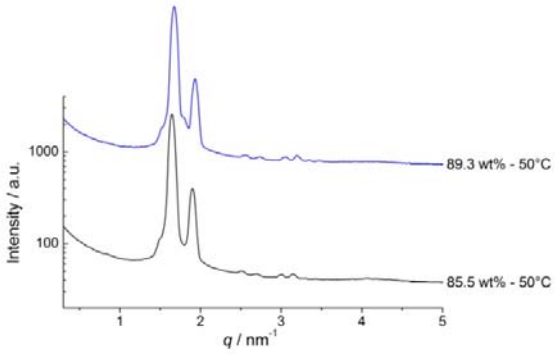

IV.3.5. Lamellar phase L_α

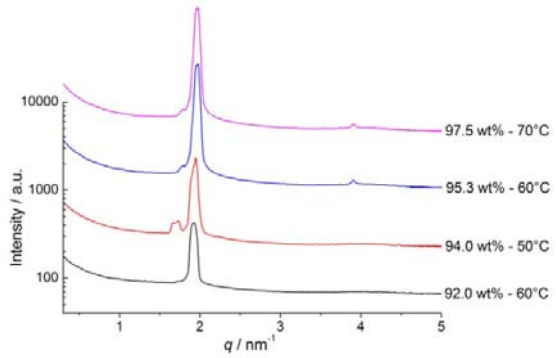

IV.4. ChC18

IV.4.1. Hexagonal phase H_1

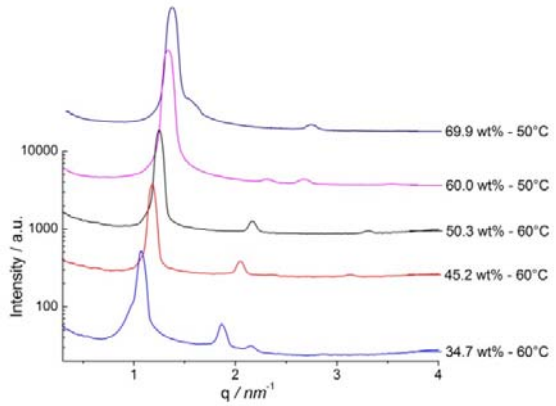

IV.4.2. Bicontinuous phase V_1 with I*a3d* structure

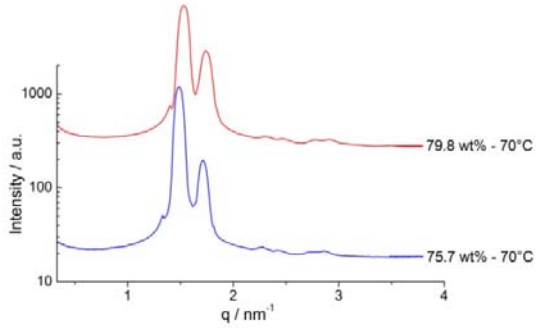

IV.4.3. Lamellar phase L_α

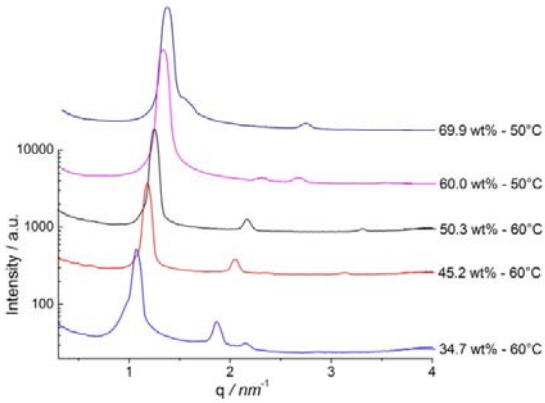

V. X-ray data and phase assignment

V.1. Attempt of assigning I_1' to $P6_3/mmc$

Clerc reported in 1996 on a new symmetry for a discontinuous cubic phase, occurring in the non-ionic system $C_{12}EO_8$.[7] The respective phase is located between the micellar solution and an I_1 phase of P*m3n* structure. It consists of two micelles per unit cell arranged in a hexagonal compact structure of space group $P6_3/mmc$ and is nonetheless of isotropic nature. The ratio $R = c/a$ of the hexagonal unit cell indicated that the micelles are of quasi-spherical shape. Afterwards, Zeng *et al.* confirmed in 2007 that this isotropic phase is constructed of hexagonal close packed (hcp) perfectly spherical micelles.[8]

Assuming that the $P6_3/mmc$ structure reflects the basic lattice of I_1', the unit cell parameter a is given by:[7]

$$a = d\sqrt{4/3\left(h^2+k^2+hk\right)+l^2/R^2}$$

By trying different values for 35.1 wt% ChC12, for instance, we found the lowest statistical error for R= 1.635, which is very close to those of a hexagonal close compact packing of spheres (R= 1.633). The volume of the hexagonal unit cell is given by:[7]

$$V_{Unitcell} = \frac{\sqrt{3}}{2} Ra^3$$

Knowing the volume fraction of surfactant Φ_S and the volume of one surfactant molecule V_S, the micelle aggregation N_{agg} with respect to two micelles per unit cell can be calculated according to:

$$N_{agg} = \left(V_{Unitcell} \cdot \Phi_S / V_S\right)/2$$

Therewith, we derive for 35.1 wt% ChC12 to a= 51.3 ± 0.8 Å and to $V_{Unit\ cell}$= 191 381 Å^3, resulting in an aggregation number of N_{agg} = 66.0.

V.2. X-ray data of I_1''

Table 5 lists the X-ray diffraction data obtained on I_1'' for different *m* values of choline soaps. Unfortunately data on I_1'' of ChC18 are missing at the moment due to limited facilities.

	I_1'' – P*m3n*							
	ChC12	ChC12	ChC12	ChC12	ChC14	ChC14	ChC14	ChC16
wt%	37.9	40.1	45.0	47.2	34.9	37.4	40.9	34.8
Φ_S	0.383	0.405	0.455	0.477	0.356	0.381	0.416	0.358
d_{110}/Å	-	-	62.8	62.2	-	73.9	74.8	-
d_{200}/Å	45.5	45.2	44.6	44.2	53.2	52.8	52.4	62.2
d_{210}/Å	40.5	40.0	39.8	39.5	47.6	46.9	46.9	55.6
d_{211}/Å	37.2	36.7	36.1	36.6	42.5	43.0	43.6	51.1
d_{220}/Å	32.2	31.7	31.6	31.3	37.0	37.2	38.1	44.6
d_{310}/Å	-	28.6	28.2	28.0	-	34.0	34.1	39.3
d_{222}/Å	26.4	26.0	25.5	25.5	31.0	30.8	31.0	35.7
d_{320}/Å	25.5	24.9	24.6	24.5	-	29.8	29.8	34.9
d_{321}/Å	24.5	24.0	23.7	23.6	28.2	28.6	28.7	33.4
d_{400}/Å	-	22.4	22.2	-	26.5	26.7	-	31.4
d_{410}/Å	-	21.8	21.5	-	25.9	25.9	26.0	30.2
$d_{330+411}$/Å	-	21.0	20.9	20.8	-	-	-	-
a /Å	91.3 ± 0.5	89.9 ± 0.3	88.8 ± 0.2	88.4 ± 0.4	105.8 ± 1.1	106.1 ± 1.0	106.7 ± 1.2	124.9 ± 0.8
N_{agg}	70.9	71.4	77.4	79.8	92.7	100.1	111.1	139.4

Table 5. X-ray diffraction data of ChC*m* salts up to *m*= 16 at 25°C with P*m3n* structure. The table comprises the volume fraction of surfactant Φ_S, the experimental *d*-values with the corresponding *Miller* indices, the resulting unit cell parameter *a* and the aggregation numbers N_{agg}, which have to be considered as rough approximations. 37.9 wt% ChC12 and 34.9 wt% ChC14 are biphasic samples of I_1' and I_1'', while 47.2 wt% ChC12 is located in the two phase region of I_1'' and H_1.

V.3. X-ray data of H_1

Table 6 lists the X-ray diffraction data of H_1 obtained for the different alkyl chain lengths of choline soaps. Towards higher surfactant concentrations, some reflections are systematically suppressed. For instance, the intensity of the *110* reflection tends to zero, while that of the *200* reflection passes through a minimum, similar to the report by Luzzati and coworkers for alkali soaps.[9]

	Hexagonal – H_1									
	wt%	Φ_S	*T* /°C	d_{100} /Å	d_{110} /Å	d_{200} /Å	d_{210} /Å	d_{300} /Å	d_{220} /Å	*a* /Å
ChC12	49.7	0.502	25	36.7	21.3	18.5	14.0	-	-	42.6 ± 0.1
	55.1	0.556	25	36.1	21.1	18.1	13.8	-	-	41.9 ± 0.2
	60.2	0.606	25	35.1	20.3	-	13.3	-	10.1	40.6 ± 0.1
	65.5	0.659	25	34.3	19.9	-	13.0	-	-	39.8 ± 0.1
	69.9	0.703	25	33.8	19.5	17.0	12.8	-	-	39.1 ± 0.1
	74.7	0.750	25	33.1	19.2	16.6	-	-	-	38.3 ± 0.1
	79.9	0.802	25	32.6	-	16.3	-	10.9	-	37.7 ± 0.1
	83.8	0.840	25	32.2	-	16.2	-	10.8	-	37.3 ± 0.1
ChC14	45.0	0.457	25	43.3	25.1	21.7	16.3	-	-	50.1 ± 0.2
	50.6	0.513	25	41.9	24.2	21.1	15.9	-	-	48.5 ± 0.2
	56.0	0.567	25	40.3	23.4	20.3	15.3	-	-	46.7 ± 0.1
	61.0	0.618	25	39.0	22.8	-	14.9	-	-	45.3 ± 0.2
	70.2	0.708	25	37.2	21.4	18.6	-	12.4	-	43.0 ± 0.1
	75.4	0.759	25	36.7	21.2	18.5	-	12.3	-	42.6 ± 0.2
	79.8	0.803	25	35.9	-	18.0	-	12.0	-	41.6 ± 0.1
ChC16	40.1	0.411	25	51.5	29.8	25.8	19.5	-	-	59.5 ± 0.1
	45.2	0.463	25	49.5	28.4	24.8	18.7	16.6	-	57.2 ± 0.2
	49.7	0.510	25	47.6	27.3	23.8	17.9	-	13.2	54.8 ± 0.2
	54.7	0.557	25	45.9	26.5	-	17.5	-	13.3	53.1 ± 0.2
	59.6	0.606	25	44.6	25.8	22.4	16.9	-	12.9	51.6 ± 0.2
	64.4	0.654	25	43.6	25.1	21.8	16.5	-	12.7	50.4 ± 0.2
	69.7	0.706	25	42.7	24.7	21.6	-	14.3	12.4	49.5 ± 0.2
ChC18	34.7	0.359	60	58.7	33.8	29.2	-	-	-	67.6 ± 0.2
	45.2	0.465	60	53.2	30.6	26.7	20.1	-	-	61.5 ± 0.2
	50.3	0.516	60	50.3	29.0	-	19.0	-	-	58.0 ± 0.1
	60.0	0.612	50	46.9	27.2	23.4	17.7	-	-	54.2 ± 0.1
	69.9	0.710	50	45.5	-	22.9	-	-	-	52.8 ± 0.3

Table 6. X-ray diffraction data for the hexagonal phase H_1 of ChC*m* soaps with *m*= 12-18, including the volume fraction of surfactant Φ_S, the temperature *T*, the experimental *d*-values with the assignment to the corresponding Miller indices and the therewith resulting unit cell parameters *a*. 83.8 wt% ChC12 represents possibly a biphasic sample, as shown in the following chapter.

V.4. H_1 - V_1 boundary: Intermediate phase?

As mentioned in the main text, additional reflections occur close to the phase boundary of H_1/ V_1. Indeed, these have been not observed for ChC14, but which can most probably be attributed to the lower resolution of the experimental setup used for ChC14.

Table 7 shows the attempt of assigning the additional reflections to an intermediate phase of complex hexagonal structure (ribbon phase with of *cmm* symmetry). Compared to the other liquid crystalline phases, the peak positions are much less sensitive towards concentration variations, but are still shifted to lower scattering angles when elongating the alkyl chain.

	H_1 / V_1 – complex hexagonal							
	wt%	Φ_S	T /°C	d_{100} /Å	d_{110} /Å	d_{200} /Å	d_{210} /Å	a /Å
ChC12	83.8	0.840	25	39.5	22.8	19.8	15.0	45.7 ± 0.1
	86.9	0.871	25	39.3	22.8	19.7	14.9	45.5 ± 0.2
	89.5	0.897	25	38.8	22.6	-	-	45.0 ± 0.3
ChC16	74.8	0.756	60	47.6	27.6	23.9	18.1	55.1 ± 0.1
	79.3	0.800	50	47.2	27.2	23.6	17.8	54.5 ± 0.1
ChC18	79.8	0.806	70	51.1	29.6	25.8	-	59.2 ± 0.2

Table 7. X-ray diffraction data of choline soaps near the phase boundary H_1 / V_1. Each sample represents a biphasic system of possibly an intermediate phase of complex hexagonal structure and H_1 (83.8 wt% ChC12 and 74.8 wt% ChC16) or V_1 (remaining probes), respectively. The table includes the volume fraction of surfactant Φ_S, the temperature *T*, the experimental *d*-values with the for a 2-D hexagonal lattice corresponding *Miller* indices, and the unit cell parameter *a*.

Alternatively, the additional peaks can be fitted by a cubic lattice, namely $I4_132$, which exhibits Bragg spacing ratios of √2 : √6 : √8 : √10 : √12 (see Table 8). The statistical error of the $I4_132$ unit cell is only slightly larger as for a 2-D hexagonal lattice, but the *310* and *222* reflections are missing in all instances.

	H_1 / V_1 – $I4_132$									
	wt%	Φ_S	T /°C	d_{110} /Å	d_{211} /Å	d_{220} /Å	d_{310} /Å	d_{222} /Å	d_{321} /Å	a /Å
ChC12	83.8	0.840	25	39.5	22.8	19.8	-	-	15.0	56.0 ± 0.1
	86.9	0.871	25	39.3	22.8	19.7	-	-	14.9	55.8 ± 0.2
	89.5	0.897	25	38.8	22.6	-	-	-	-	55.1 ± 0.4
ChC16	74.8	0.756	60	47.6	27.6	23.9	-	-	18.1	67.5 ± 0.1
	79.3	0.800	50	47.2	27.2	23.6	-	-	17.8	66.7 ± 0.1
ChC18	79.8	0.806	70	51.1	29.6	25.8	-	-	-	72.6 ± 0.3

Table 8. X-ray diffraction data of choline soaps near the phase boundary H_1 / V_1. Each sample represents a biphasic system of eventually a cubic $I4_132$ structure and H_1 (83.8 wt% ChC12 and 74.8 wt% ChC16) or V_1 (remaining samples), respectively. The table includes the volume fraction of surfactant Φ_S, the temperature *T*, the experimental *d*-values with the corresponding *Miller* indices for $I4_132$, and the unit cell parameter *a*.

V.5. Bicontinuous cubic phase V_1

	V_1 – I*a3d*									
	wt%	Φ_S	T /°C	d_{211}/Å	d_{220}/Å	d_{321}/Å	d_{400}/Å	d_{420}/Å	d_{332}/Å	a /Å
ChC12	86.9	0.871	25	31.1	27.0	-	-	-	-	76.2 ± 0.1
	89.5	0.897	25	30.8	26.7	20.3	-	-	-	75.6 ± 0.2
	91.5	0.916	25	30.4	26.4	20.0	18.7	16.7	15.9	74.6 ± 0.2
	94.0	0.941	25	30.2	26.1	19.9	18.5	16.5	15.8	74.0 ± 0.2
	97.5	0.975	60	29.0	25.0	19.0	17.9	15.9	15.1	71.1 ± 0.2
ChC14	79.8	0.803	60	34.0	29.4	-	-	-	-	83.1 ± 0.1
	83.3	0.837	25	35.1	30.7	-	-	-	-	86.3 ± 0.5
	85.5	0.859	20	34.5	30.1	-	-	-	-	84.8 ± 0.3
	90.4	0.906	25	33.6	29.2	22.1	20.6	18.5	17.6	82.6 ± 0.3
	93.2	0.934	35	32.9	28.7	21.6	20.2	18.0	17.2	80.7 ± 0.3
	95.1	0.952	45	32.4	28.3	21.3	19.9	17.7	17.1	79.7 ± 0.4
ChC16	79.3	0.800	50	39.0	33.9	25.8	-	21.4	20.3	95.8 ± 0.4
	85.5	0.860	50	38.1	33.1	25.0	23.4	20.9	19.9	93.4 ± 0.2
	89.3	0.897	50	37.6	32.6	24.6	23.0	20.5	19.6	92.1 ± 0.1
ChC18	75.7	0.766	70	42.2	36.7	27.6	25.8	23.1	22.0	103.3 ± 0.3
	79.8	0.806	70	41.1	35.9	27.2	25.4	22.7	21.6	101.4 ± 0.4

Table 9. X-ray diffraction data for V_1 of ChC*m* soaps with I*a3d* structure, listing the volume fraction of surfactant Φ_S, the temperature T, the experimental d-values with the assignment to the corresponding *Miller* indices and the unit cell parameter a. Samples of ChC12 up to 89.5 wt%, 79.3 wt% ChC16 and 75.7 wt% ChC18 are potentially biphasic as discussed in the former chapter.

Figure 8 shows that the decrease of the unit cell towards higher soap concentrations.

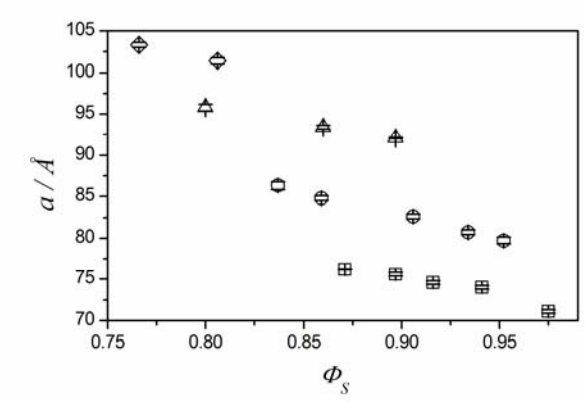

Figure 7. V_1 phase of ChC*m* salts: unit cell parameter a of the I*a3d* structure versus the volume fraction of surfactant Φ_S, showing the different alkyl chain lengths in comparison (ChC12 (□), ChC14 (○), ChC16 (△) and ChC18 (◇)) at temperatures as in Table 9.

References

1. C. Tanford, *J. Phys. Chem.*, 1972, **76**, 3020-3024.
2. S. Fouilloux, A. Desert, O. Tache, O. Spalla, J. Daillant and A. Thill, *J. Colloid Interface Sci.*, 2010, **346**, 79-86.
3. T. Zemb, O. Tache, F. Ne and O. Spalla, *Rev. Sci. Instrum.*, 2003, **74**, 2456-2462.
4. T. C. Huang, H. Toraya, T. N. Blanton and Y. Wu, *J. Appl. Crystallogr.*, 1993, **26**, 180-184.
5. V. Urban, P. Panine, C. Ponchut, P. Boesecke and T. Narayanan, *J. Appl. Crystallogr.*, 2003, **36**, 809-811.
6. T. N. Blanton, C. L. Barnes and M. Lelental, *J. Appl. Crystallogr.*, 2000, **33**, 172-173.
7. M. Clerc, *J. Phys. II*, 1996, **6**, 961-968.
8. X. Zeng, Y. Liu and M. Imperor-Clerc, *J. Phys. Chem. B*, 2007, **111**, 5174-5179.
9. F. Husson, H. Mustacchi and V. Luzzati, *Acta Crystallogr.*, 1960, **13**, 668-677.